

Q. Yang · S. Goding · M. Hagenaars · T. Carlos  
P. Albertsson · P. Kuppen · U. Nannmark  
M. E. Hokland · P. H. Basse

## Morphological appearance, content of extracellular matrix and vascular density of lung metastases predicts permissiveness to infiltration by adoptively transferred natural killer and T cells

Received: 8 April 2005 / Accepted: 9 June 2005 / Published online: 27 July 2005  
© Springer-Verlag 2005

**Abstract** We have recently shown that adoptively transferred, IL-2-activated natural killer (A-NK) cells are able to eliminate well-established B16-F10.P1 melanoma lung metastases. However, some B16-F10.P1 lung metastases were resistant to infiltration by the A-NK cells and also resistant to the A-NK cell treatment. The infiltration-resistant (I-R) B16-F10.P1 metastases had a unique “compact” morphology compared to the “loose” morphology of the infiltration-permissive (I-P) metastases. Here, we show that I-P loose tumors and I-R compact tumors are also found in lung metastases of mouse Lewis lung carcinoma (3LL), MCA-102 sarcoma, and MC38 colon carcinoma as well as rat MADB106 mammary carcinoma origin. Furthermore, the infiltration resistance of the compact tumors is not restricted to A-NK cells, since PHA and IL-2 stimulated CD8+ T-cells (T-LAK cells) also infiltrated the compact tumors poorly. Analyses of tumors for extracellular matrix (ECM) components and PECAM-1<sup>+</sup> vasculature, revealed that the I-R lesions are hypovascularized and contain very little laminin, collagen and fibronectin. In contrast, the I-P loose tumors are well-vascularized and they contain high amounts of ECM components. Interestingly, the distribution pattern of ECM components in the I-P loose

tumors is almost identical to that of the normal lung tissue, indicating that these tumors develop around the alveolar walls which provide the loose tumors with both a supporting tissue and a rich blood supply. In conclusion, tumor infiltration by activated NK and T cells correlates with the presence of ECM components and PECAM-1<sup>+</sup> vasculature in the malignant tissue. Thus, analysis of the distribution of ECM and vasculature in tumor biopsies may help select patients most likely to benefit from cellular adoptive immunotherapy.

**Keywords** Natural killer cells · Immunotherapy · Lung metastases · Extracellular matrix-homing

**Abbreviations** IL-2: Interleukin-2 · A-NK: Activated natural killer · Peg: Polyethylene glycol · NK: Natural killer · 3LL: Lewis lung carcinoma · ECM: Extracellular matrix

### Introduction

Natural killer (NK) cells are usually found only in low numbers in tumors and tumor metastases. However, following activation either in vivo [12] or ex vivo [10, 19, 26] with IL-2 and other biological response modifiers, the NK cells [4, 12] as well as CD8+ T cells [13] acquire the ability to localize selectively at tumor sites. Once in the tumor tissue, the activated NK (A-NK) cells are able to establish contact with the tumor cells [5] and to kill these [27]. However, an efficient killing of solid, well-established tumors only takes place if a certain number of the killer cells reach the tumor tissue [27]. Thus, as recently reviewed [1], successful localization of the A-NK cells into tumors is a prerequisite for anti-tumor effect.

While tumor-localization by IL-2-activated NK cells has been demonstrated in both the B16-F10.P1 [4] and Lewis lung carcinoma [27] models in mice and in the CC531 colon carcinoma [16, 23] and MADB106

Q. Yang · S. Goding · T. Carlos · P. H. Basse (✉)  
University of Pittsburgh Cancer Institute,  
Hillman Cancer Center G17a, University of Pittsburgh,  
5117 Centre Avenue, Pittsburgh, PA 15213, USA  
E-mail: basse@imap.pitt.edu  
Tel.: +1-412-6233236  
Fax: +1-412-6231119

M. Hagenaars · P. Kuppen  
University of Leiden, Leiden, Holland

P. Albertsson  
Department of Oncology, Sahlgren University Hospital,  
Göteborg, Sweden

U. Nannmark  
University of Göteborg, Göteborg, Sweden

M. E. Hokland  
Institute of Medical Microbiology,  
University of Aarhus, Aarhus, Denmark

mammary carcinoma models in rats [22], it appears that some tumor nodules, even within the same organ, are more resistant to NK cell infiltration than other nodules. In the B16-F10.P1 melanoma model, we have shown that the infiltration-resistant (I-R) and -permissive nodules in the lung tissue grow with distinct morphologies. The infiltration-permissive (I-P) tumors are located in the lung parenchyma and seem to infiltrate the surrounding lung tissue in all directions, generating a diffuse and irregular demarcation to the normal lung tissue. The structure of these tumors appears loose (therefore named “loose” tumors) and these tumors appear to contain a relatively high amount of non-B16-F10.P1, host tissue components [21]. In contrast, the I-R nodules almost always grow around a tubular structure (blood vessels or parts of the bronchial tree) and form sharp lines of demarcation to the surroundings. Morphologically, these nodules are very dense (therefore named “compact” tumors) and appear to be composed almost exclusively of tumor cells. As expected, the I-P, loose tumors respond more efficiently to adoptive A-NK cell therapy than the compact, I-R tumors [27].

To be able to direct immune effector cells such as NK and T cells to all tumor nodules regardless of their morphologic type, the basis for the resistance of the compact nodules needs to be further investigated. Here, we have focused on the expression of extracellular matrix components and vascular markers in loose and compact tumors of different histologic origins and the possible correlation between the presence of these components and permissiveness to infiltration by IL-2 and IL-2 plus PHA activated NK and CD8<sup>+</sup> T cells (T-LAK cells), respectively. Since few adoptively transferred effector cells are found in the circulation beyond the initial 24 h after injection [20], we focused our analysis of tumor-localization by NK and T-cell derived effector cells at the 24 h time point.

## Materials and methods

### Animals and tumor cell lines

Female C57BL/6 and congenic B6.Pl-Thy-1<sup>a</sup>Cy mice, 8–12 weeks of age, were obtained from Jackson (Bar Harbor, ME, USA). Fisher 344 rats were obtained from Harlan (Indianapolis, IN, USA). The use of animals for the experiments described below was approved by the Institutional Animal Care and Use Committee, University of Pittsburgh. The subline F10.P1 of the B16 melanoma (C57BL/6 origin) was established in our laboratory from a B16-F10 lung metastasis and was maintained in RPMI-1640 medium (Life Technologies, Gaithersburg, MD, USA) supplemented with 10% heat inactivated fetal calf serum, 2 mM glutamine, 20 mM Hepes buffer, 0.8 g/l streptomycin and 1.6×10<sup>5</sup> U/l penicillin. Lewis lung carcinoma (3LL) was obtained from ATCC. MCA-102 was a kind gift from Dr. E. Gorelik, University of Pittsburgh, the MC38 colon

carcinoma was a gift from Dr. M. Shurin, University of Pittsburgh, and the rat mammary carcinoma MADB106 was obtained from Dr. W. Chambers, University of Pittsburgh. Adherent cells were detached by exposure to 0.02% EDTA for 2–3 min and washed three times in RPMI-1640. Cell viability, judged by trypan blue dye exclusion test, was always >95%. Murine pulmonary metastases (B16-F10.P1, 3LL, MCA-102 and MC38) were established by tail vein injection of 0.2–0.4×10<sup>6</sup> cells in 0.3 ml of RPMI-1640 into C57BL/6 mice, pretreated on day<sup>-1</sup> with 40 μl anti-asialoGM1 antiserum (Wako Pure Chemicals, Wako, TX, USA). MADB106 pulmonary metastases were established by injection of 0.4×10<sup>6</sup> cells into the lateral tail vein of Fischer 344 rats. The rats were treated with Polyinosinic-polycytidylic acid (Poly I:C) (Sigma Chemical Co., St. Louis, MO, USA). Each rat received 5 mg/kg i.p. on days 8 and 10 of tumor growth.

### A-NK and T-LAK cell preparations

Spleens were removed aseptically from congenic B6.Pl-Thy-1<sup>a</sup>Cy mice and a single-cell suspension was prepared in RPMI-1640. Erythrocytes were lysed by incubation with ammonium chloride–potassium buffer at room temperature for 3 min and the spleen cells were subsequently washed twice in RPMI-1640. Cells were transferred to T150 plastic flasks (Falcon, B&D, Franklin Lakes, NJ, USA) and cultured at 37°C in an atmosphere of 5% CO<sub>2</sub> in 50 ml of RPMI-1640 supplemented with 5% heat inactivated fetal calf serum and 5% normal human serum, 10 ml/l nonessential amino acids (Life Technologies), 50 mM 2-mercaptoethanol, 2 mM glutamine, 20 mM Hepes buffer, 0.8 g/l streptomycin and 1.6×10<sup>5</sup> u/l penicillin, hereafter referred to as complete medium (CM). To produce A-NK cells, splenocytes were stimulated with 6,000 IU/ml of human recombinant IL-2 (kindly provided by the Chiron Corporation, Emeryville, CA, USA). After 3 days of incubation, CD8-positive cells were magnetically removed following incubation of the cell culture with rat anti-CD8 antibody (TIB-105, ATCC) and subsequently with anti-rat coated magnetic beads (DynaL Biotech, Lake Success, NY, USA). The CD8-depleted cells were resuspended in fresh CM containing 6,000 IU/ml IL-2 to a final concentration of 1×10<sup>5</sup> cells/ml and returned to culture flasks. Fresh CM containing 6,000 IU/ml IL-2 was added every 2–3 days as needed. After an additional 3 days of culture, non-adherent cells were decanted and the plastic-adherent cells were harvested after a brief treatment with 0.02% EDTA and washed twice in RPMI-1640 before use. Routinely, these A-NK cells were >95% Thy1.1<sup>+</sup>, >95% asGM1<sup>+</sup>, >90% NK1.1<sup>+</sup>, <2% CD8<sup>+</sup>, <2% CD4<sup>+</sup>. To produce T-LAK cells, splenocytes were transferred to T150 plastic flasks at 2×10<sup>5</sup> cells/ml of complete medium. The cells were activated with 600 IU/ml of rhIL-2 and 8 μg/ml of PHA-P (phytohemagglutinin-P; DIFCO, Detroit, MI,

USA). After 2 days of incubation, clusters of T cells were transferred to 50 ml tubes and sediments were allowed to form for 5–7 min before the supernatant was gently removed. The cell sediment was resuspended at  $1 \times 10^5$  cells/ml of fresh CM medium containing 600 IU IL-2/ml. Three days later, the cells were harvested, washed twice, and resuspended in RPMI-1640. Routinely, the T-LAK cells were found to be  $>95\%$  Thy1.1<sup>+</sup>,  $>95\%$  asialo-GM1<sup>+</sup>,  $>90\%$  CD8 (Lyt-2)<sup>+</sup>,  $>90\%$  CD3<sup>+</sup>, but  $<5\%$  NK1.1<sup>+</sup> and  $<2\%$  CD4 (L3T4)<sup>+</sup>, in agreement with previous findings [13].

#### Adoptive transfer of A-NK and T-LAK cells

Seven to ten days after induction of pulmonary metastases in C57BL/6 mice, intravenous (i.v.) inoculation of 10 million A-NK or T-LAK cells in 300  $\mu$ l of PBS was performed via the lateral tail vein. To support the transferred cells, animals received i.p. injections of 0.5 ml RPMI containing 60,000 IU IL-2 complexed to polyethylene glycol (PEG-IL-2, a kind gift from the Chiron Corporation, Emeryville, CA, USA) at 0 and 12 h after the cell injection. Lungs and other organs were removed at different time points after the adoptive transfer and processed as described below.

#### Identification of lung metastases subtypes

The subtype of individual lung metastases were classified according to morphologic appearance (loose (L) or compact (C)) as previously described [21]. Briefly, *loose* (L) metastases are found deeper in the lung tissue surrounded by normal tissue on all sides. The loose metastases often appear spherical in shape but their demarcation to the surrounding tissue is poorly defined. Alveolar cells, lymphocytes and granulocytes are found in these metastases and various amounts of extracellular tissue are seen in between the melanoma cells. *Compact* (C) metastases have a distinct line of demarcation to the surrounding tissue and they grow in an expansive fashion. These metastases are mostly found growing in a sleeve-like pattern around larger tubular structures, such as arterioles and bronchioles. On cross-sections, these metastases often appear bigger than the loose metastases indicating a high growth potential.

#### Estimation of A-NK and T-LAK cell infiltration of lung metastases

Lung tissue as well as other tissues from each animal were snap-frozen at  $-70^\circ\text{C}$  in *n*-Hexane. Eight micrometer thick sections from 3 to 5 different areas from each set of lungs were randomly chosen and the sections were stained by one- or two-layer immunofluorescence technique. Briefly, after fixation of the tissue sections in acetone for 5 min, the slides were washed twice

( $2 \times 5$  min) in PBS buffer containing 1% FCS. PE-conjugated, rat monoclonal anti-Thy1.1 antibody (OX-7, BD Bioscience, Pharmingen, San Diego, CA, USA) was used in a 1:100 dilution. PE-conjugated rat IgG2b (A95-1, BD Bioscience) was used as a control. Anti-PECAM-1 antibody (MEC 13.3, Pharmingen) was used in 1:100 dilution. Polyclonal rabbit anti laminin (EY Laboratories, USA), fibronectin (PAB468, Maine Biotechnology Services) and collagen antibodies (PAB467, Maine Biotechnology Services) were used in a 1:100 dilution. A 1:50 dilution of PE- or FITC-conjugated goat anti-rabbit antibodies (from Molecular Probes, Eugene, OR, USA, and ICN Biomedicals Inc, Aurora, OH, USA, respectively) were used as second-layer antibody. Normal rabbit serum was used as control. Sections were incubated with each antibody in a humidified chamber for 30 min at room temperature and washed twice in COONs buffer supplemented with 1% FCS.

#### Estimation of density of A-NK and T-LAK cells, vasculature and ECM components

The density of positively stained cells (A-NK and T-LAK cells, endothelial cells) and ECM components (laminin, collagen and fibronectin) was measured by image analysis using MetaMorph software (Universal Imaging Corporation, Downingtown, PA, USA). From each set of lungs (3–4 mice per group), at least 12 tumors of each phenotype and twelve 0.25 sq mm areas of normal tissue (found in 3–5 sections sampled at random from all areas of the lungs) were analyzed. The density of ECM components and vasculature is expressed as percent area. In areas of tumors and normal tissue where individual A-NK and T-LAK cells could easily be identified, the average number,  $\bar{x}$ , of PE-positive pixels associated with each A-NK and T-LAK cell was calculated. Based on this value, the number of effector cells in tumors and normal tissue could be estimated as: number of PE-positive pixels in area of interest divided by  $\bar{x}$ .

## Results

#### Morphology of B16-F10.P1, 3LL, MCA-10 2 and MC38 lung metastases

Following i.v. injection, tumor cells of B16-F10.P1, 3LL, MCA-102 and MC38 origin formed metastases of two distinct morphologies (Fig. 1). Most metastases (75% to  $>90\%$ ) were composed of loosely connected tumor masses containing a varying degree of infiltrating host leukocytes. The border to the surrounding normal tissue was poorly defined (Fig. 1-top panels). In contrast, a smaller number of metastases were composed of a compact mass of tumor tissue containing very few infiltrating host cells. Most of these tumors grew as sheets along and around tubular structure of the lungs (vessels or bronchi) and their border to the surrounding



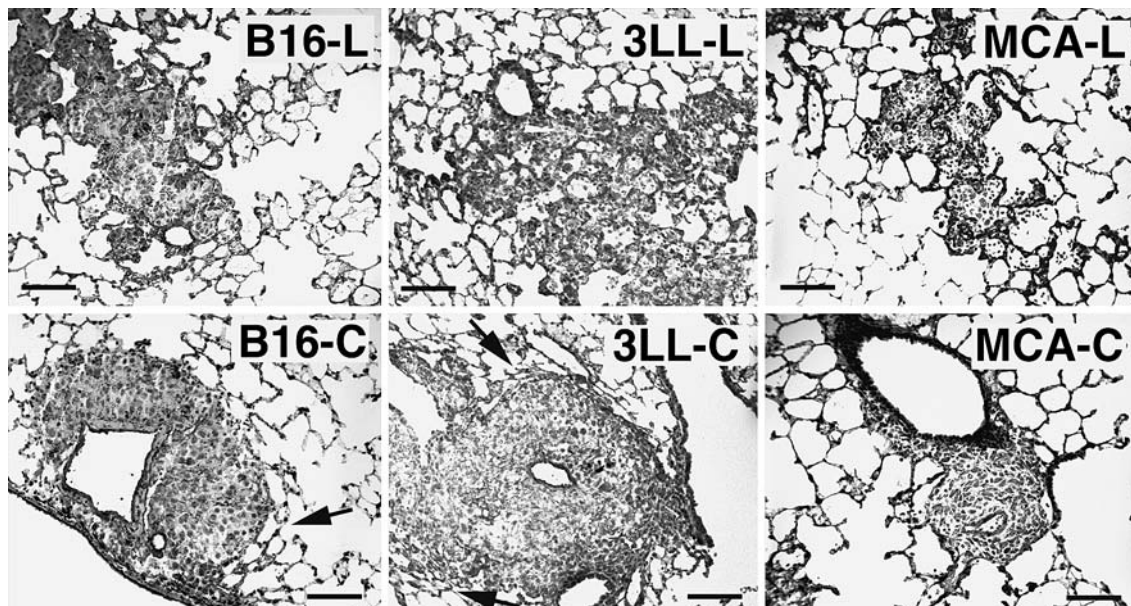


**Fig. 1** Morphology of B16-F10.P1, 3LL and MCA-102 lung metastases.  $3 \times 10^5$  tumor cells of B16-F10.P1, 3LL and MCA-102 origin were injected via the lateral tail vein. Twelve days later, lungs were removed and snap frozen. Cryosections were produced and stained with hematoxylin. In all three tumor models, tumors of similar morphology were identified; loose tumors (*top row*; B16-L, 3LL-L and MCA-L) had irregular borders to the surrounding normal lung tissue and seemed to grow around the alveolar walls and into the alveolar spaces. Compact tumors (*bottom row*; B16-C, 3LL-C and MCA-C) had a sharp line of demarcation, compressed the surrounding normal lung tissue (*arrows* in B16-C and 3LL-C) and almost always surrounded a tubular structure of the lungs (most often medium to large vessels). *Bars* indicate 100  $\mu$ m

normal tissue was well-defined (Fig. 1-bottom panels). The growth rate of the compact tumor nodules seemed to be slightly faster than that of the loose type of metastases, as judged by the average tumor size at day 12–15 after induction. While the compact type of tumors seemed to grow by expansion (and often with compression of the surrounding lung tissue—arrows in Figs. 1 and 2A-a), the loose type of metastases seemed to invade and grow into the alveolar sacs of the lung tissue (Fig. 2A-b). The compact type of metastases was seen at the highest frequency (15–25%) in the B16-F10.P1 model and less frequently (5–10%) in the MCA-102 and MC38 models.

#### Ability of adoptively transferred A-NK and T-LAK cells to infiltrate compact and loose metastases

We have previously shown that while adoptively transferred A-NK cells are able to localize in high numbers into B16-F10.P1 lung metastases of the loose phenotype at 24 h after i.v. injection, they reach lung metastases of the compact phenotype in much lower numbers [21]. Similarly, analysis of localization of endogenous NK cells, identified by staining with anti-CD161 antibody, into MADB106 lung metastases following treatment with

the biological response modifier polyI:C demonstrated that endogenous NK cells also localize less efficiently into compact than loose metastases (Fig. 2B). To evaluate whether this is a general phenomenon, the localization of A-NK cells as well as T-LAK cells into compact and loose metastases of 3LL and MCA-102 origin was measured at 24 h after injection. This experiment revealed that also in the 3LL, MCA-102 and MC38 models, A-NK and T-LAK cells localized to a significantly higher extent into metastases of the loose than the compact phenotype (Fig. 2C). While the density of A-NK cells and T-LAK cells in the compact tumors was equally low, the density of A-NK cells in the loose tumors was in general higher than that of T-LAK cells.

#### Correlation between metastasis phenotype, content of extracellular matrix and vasculature, and A-NK and T-LAK cell infiltration

The ability of immune effector cells such as NK and T-cells to migrate into tumor nodules is likely to be dependent on the abundance of vasculature and/or extracellular matrix (ECM) in the tumor. To evaluate the amount of ECM and vasculature in lung metastases, tissue sections were stained with antibodies against laminin (Fig. 2A, B, D–F), collagen, fibronectin and the vascular marker PECAM-1 (Fig. 2F) and the density of these components in compact and loose tumors was measured. Clearly, the loose type of metastases of B16-F10.P1, 3LL, MC38 and MCA-102 origin contained significantly more ( $P < 0.05$ ) of these components than the compact tumors (Figs. 3 and 4). Interestingly, while the density of laminin (Fig. 3), PECAM-1<sup>+</sup> vasculature (Figs. 2F and 4a) and fibronectin and collagen (Fig. 4b) in the compact metastases was several fold below that of the normal lung tissue, the loose tumors contained almost the same amount of these components as the

normal lung tissue. In addition, the distribution pattern of laminin and the other ECM and vascular components in the loose tumors was surprisingly similar to that of the surrounding normal tissue (Fig. 2Ea + c).

## Discussion

Localization of A-NK cells, T cells, and probably other immune effector cells as well, to sites of tumor growth is thought to be a prerequisite for anti-tumor effect. While the ability of adoptively transferred A-NK and T cells to traffic to tumor sites has been clearly demonstrated by us [4, 13, 27] and others [14, 15], we have found, in the B16-F10.P1 tumor model, that individual tumor nodules, even when located in the same organ and at close proximity, differ with respect to permissiveness to infiltration [4, 27]. This difference was found to correlate with the morphologic appearance—loose or compact—of the nodules [21]. Here, we demonstrate that not only tumor cells of B16-F10.P1 origin, but also of mouse 3LL, MCA102 sarcoma and MC38 colon carcinoma, and of rat MADB106 mammary carcinoma origin are capable of inducing both loose and compact lung tumor nodules that are NK/T-LAK cell-infiltration permissive and resistant, respectively. Thus, the correlation between tumor morphology (compact versus loose) and A-NK/T-LAK cell infiltration is not restricted to the B16-F10.P1 model, but appears to be a general phenomenon.

We hypothesized that the difference in permissiveness to effector cell infiltration between the compact and loose tumors was related to differences in extra cellular matrix composition between these two tumor types. To test this hypothesis, we compared their content of the ECM components laminin, collagen and fibronectin. The density of these components, together with the density of the vascular marker PECAM-1 were all significantly higher (three to tenfold) in loose than in compact tumors. Thus, the presence of ECM products in tumors correlates positively with the ability of immune effector cells such as A-NK and T-LAK cells to enter the tumors (correlation coefficient = 0.70). We cannot fully explain how the ECM is involved in tumor infiltration by lymphoid effector cells, but it is very likely that the ECM components are needed as a scaffold on which the A-NK and T-LAK cells can migrate. A close relationship between bundles of laminin and infiltrating NK cells was especially evident in the MADB106 rat tumor model (Fig. 2C), supporting this notion. On the other hand, especially in the B16-F10.P1 model, A-NK and T-LAK cells were often observed at some distance from the laminin bundles, indicating that these cells may not need to stay attached to the ECM components, but that they can also migrate into areas of the malignant tissue devoid of ECM components. The ECM components may serve as ligands for several of the adhesion molecules expressed by A-NK and T-LAK cells, such as VLA-4 that binds to fibronectin and the alpha-1 beta-1

**Fig. 2** A Laminin expression of compact and loose lung tumors.  $3 \times 10^5$  tumor cells of B16-F10.P1 or MADB106 origin were injected via the lateral tail vein of C57BL/6 mice and Fisher 344 rats, respectively. Twelve days later, lungs were removed and snap frozen. Cryosections were produced and stained with anti-laminin antibodies and anti-A-NK cell antibodies. **A-a** Lung section from lungs with B16-F10.P1 experimental metastases. The section was stained with rabbit anti-laminin antibody followed by peroxidase conjugated goat-anti-rabbit antibody. The section was developed with AEC substrate and counterstained with hematoxylin. Note the absence of laminin (*red staining*) in the compact (C) metastasis compared to the nearby loose (L) metastasis. *Bar* = 50  $\mu$ m. **A-b** Part of A (*enlarged*), showing growth of B16-F10.P1 cells into the alveolar spaces (*arrows*). *Bar* = 50  $\mu$ m. **B** Sections from lungs with MADB106 experimental metastases. The sections were first stained with mouse anti-3.2.3. antibody against rat NK cells. Second layer antibody was peroxidase goat anti-mouse antibody. Thereafter, the sections were stained with rabbit anti-laminin antibody followed by FITC conjugated goat-anti-rabbit antibody. The sections were developed with DAB substrate to reveal the NK cells. Note the abundance of laminin (*green fluorescence*) and NK cells (*dark dots*) in the loose (**B-a**) metastasis compared to the compact (**B-b**) metastasis. Tubular structure in compact tumor is marked with *asterisks* in (**D**). *Bars* = 50  $\mu$ m. **C** Infiltration of loose and compact B16-F10.P1, 3LL, MCA-102 and MC38 lung metastases by adoptively transferred A-NK and T-LAK cells. Density (number/sq.mm) of A-NK cells (**C-a**) and T-LAK cells (**C-b**) in loose and compact day-12 lung tumors at 24 h after injection of 15 million cells. **D** A-NK cell infiltration of loose and compact B16-F10.P1 experimental metastases. Lung sections were stained with PE-conjugated rat anti-mouse Thy1.1 antibody (to reveal adoptively transferred A-NK cells) and with rabbit anti-laminin antibody followed by FITC-conjugated goat-anti-rabbit antibody. **D-a** (overlay of DIC and green fluorescence micrographs). Note the abundance of laminin (*green fluorescence*) in the loose (L) metastases compared to the nearby compact (C) metastasis. Tubular structure in compact tumor is marked with *asterisks*. **D-b** (overlay of green and red fluorescence micrographs). Note also the high density of A-NK cells (*red fluorescence*) in the loose compared to the compact metastases. *Bars* = 50  $\mu$ m. **E** Similar distribution of laminin and PECAM-1 in loose B16-F10.P1 metastases and in normal lung tissue. Sections from lungs with B16-F10.P1 experimental metastases were stained with rabbit anti-laminin antibody followed by FITC-conjugated goat-anti-rabbit antibody, then with biotinylated rat anti-mouse PECAM-1, and finally with PE-conjugated streptavidin. **E-a** (*green fluorescence micrograph*). Note that the laminin distribution in the lungs does not reveal the presence of B16-F10.P1 lung tumors. **E-b** Overlay of DIC and green (laminin) and red (PECAM-1) fluorescence micrographs. **C** (*red fluorescence micrograph*) The PECAM-1 distribution in the lungs does not reveal the presence of B16-F10.P1 lung tumors. Note that the sections shown in (**E-b**) contain several B16-F10.P1 tumors [the darker tissue containing large amounts of melanin (*black deposits*)], indicating that the laminin and PECAM-1 found in the loose tumors is not generated by the tumor, but are remnants of the alveolar walls around which the tumor is growing. *Bars* = 50  $\mu$ m. **F** T-LAK cell infiltration of laminin<sup>+</sup>/PECAM-1<sup>+</sup> MC38 lung metastases. Lungs sections were stained with PE-conjugated anti-Thy1.1 antibody to reveal T-LAK cells. After red fluorescence micrographs were taken, the section was then stained with rabbit anti-laminin and PE-conjugated goat anti-rabbit Ig as well as with rat anti-PECAM-1 antibody and FITC-conjugated anti-rat Ig to reveal laminin and vasculature, respectively. **F-a** Hematoxylin staining of a serial section to the section shown in (**F-b-d**). **F-b** Overlay of DIC and Thy1.1 yellow fluorescence micrographs to reveal T-LAK cells. **F-c** Overlay of DIC and PECAM-1 red fluorescence micrographs to reveal vasculature. **F-d** Overlay of DIC and laminin green fluorescence micrographs to reveal laminin. *Bars* = 100  $\mu$ m



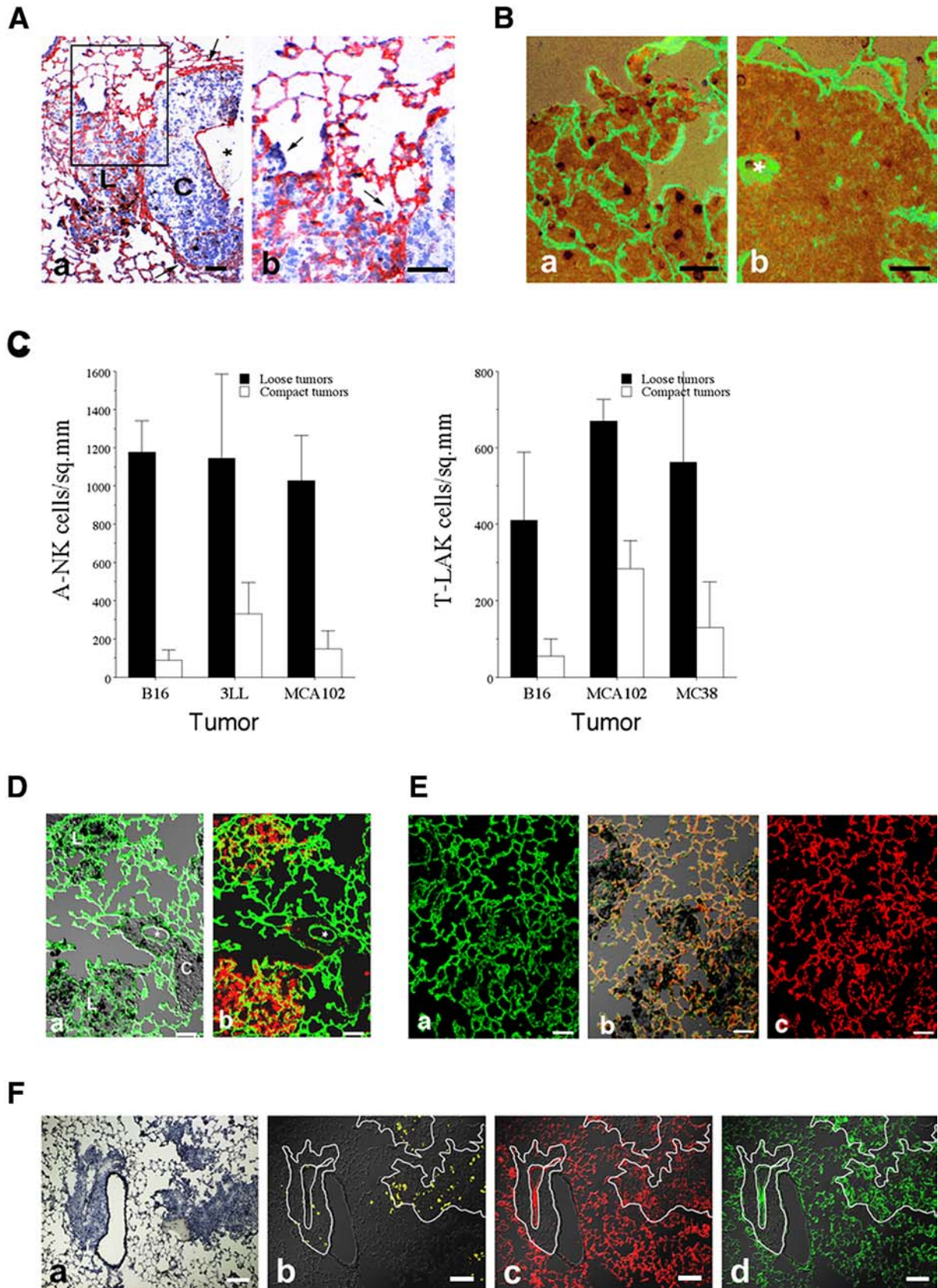


**Fig. 3** Morphology, laminin-density and density of A-NK cells and T-LAK cells in B16-F10.P1, MCA102, LEWIS LUNG, and MC38 lung metastases, respectively. The density of laminin and density of infiltrating A-NK and T-LAK cells at 24 h after injection of the effector cells was measured by image analysis of loose and compact tumors and normal lung tissue in sections stained with anti-laminin and anti-Thy1.1 antibodies

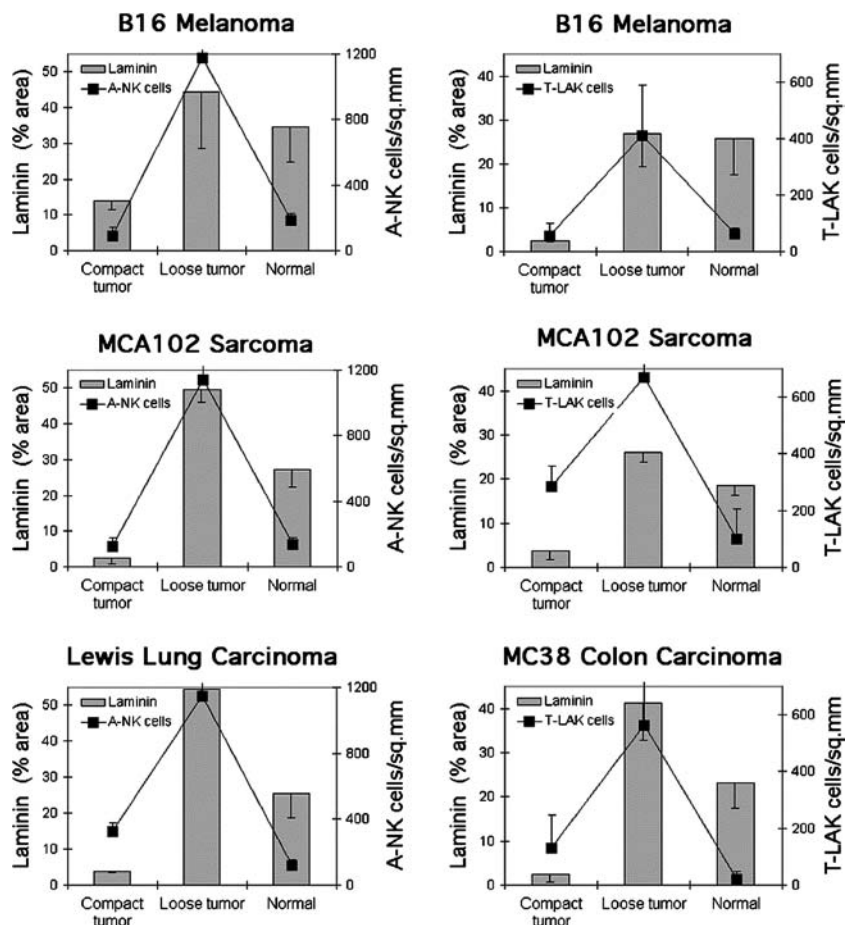
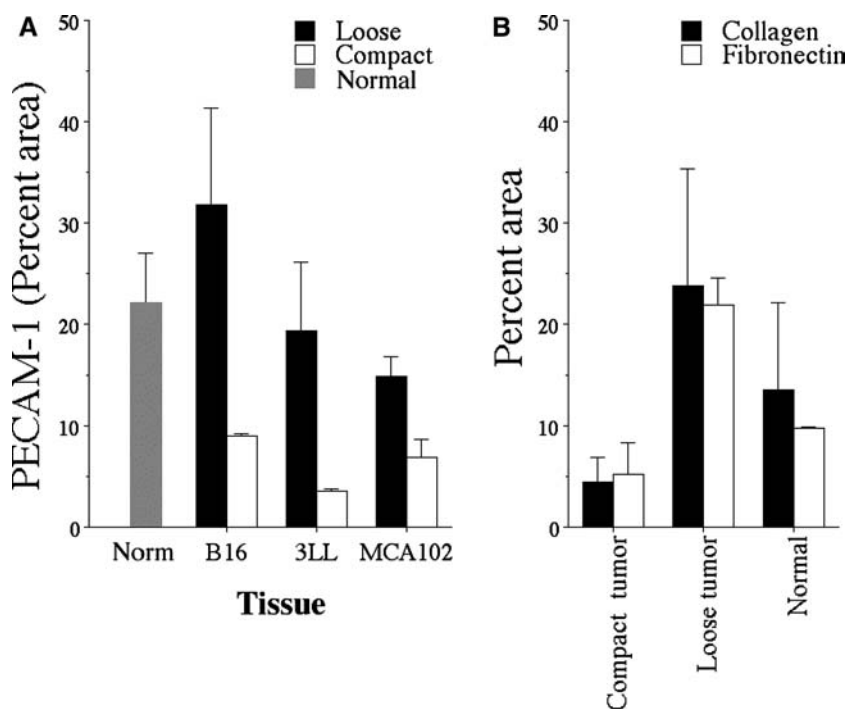


**Fig. 4** Density of collagen, fibronectin and PECAM-1 in compact and loose tumors. **a** Density of PECAM-1 in compact and loose lung tumors of B16-F10.P1, 3LL and MCA-102 origin. **b** Density of collagen and fibronectin in compact and loose lung tumors of B16-F10.P1 origin and in normal lung tissue



integrins that binds to laminin and collagen [2, 7, 17, 24]. NK cells in the decidua has been reported not to bind to laminin [6], but it is uncertain whether IL-2-activated NK cells binds laminin or not. Preliminary data indicate that A-NK cells expressing low amounts of VLA-4—obtained by FACS sorting of A-NK cells—migrate less well into loose B16-F10.P1 metastases than A-NK cells expressing higher amounts of VLA-4 (Basse and Carlos, unpublished observation). It cannot be excluded, however, that VLA-4<sup>low</sup> A-NK cells are in general less active (including migratory potential) than VLA-4<sup>high</sup> A-NK cells, and therefore are less successful in infiltrating the malignant tissues.

Another possibility is that the hypovascularization of the compact tumors—in this study illustrated by low PECAM-1 expression and in a previous studies shown by histological identification and measurement of tumor vessels [21]—would lower the chance of A-NK and/or T-LAK cells in reaching the compact tumors. While this undoubtedly is correct, we have previously shown that as many as half of the A-NK cells found in a tumor by 24 h appear to have arrived there by extravasation from smaller vessels near the tumor and migration towards and into the tumor [20]. Based on this observation, we would expect that the density of A-NK cells in the compact tumors—despite their paucity of vessels—would be close to half of that of loose tumors (due to migration of A-NK cells from the surrounding normal lung tissue). However, this is not the case (the infiltration of the compact tumors is only 10–20% of that of loose tumors). Thus, factors in addition to hypovascularization—for example, density of ECM components as argued above—must influence the permissiveness of tumors to effector cell infiltration. To further document the role of ECM components and vasculature in tumor permissiveness/resistance to infiltration, we are in the process of transfecting B16-F10.P1 cells to over-express chemotactic factors such as MIP-1a [25] and angiogenic factors such as bFGF and VEGF [3, 11, 18]. Analyses of the ability of A-NK and T-LAK cells to infiltrate compact B16-F10.P1 tumors transfected to express chemokines or angiogenic factors (i.e. compact tumors that have been “forced” to induce vessel-formation), should further clarify to what extent the presence of ECM and/or vasculature in tumors is essential for infiltration.

It is unclear why the two very distinct types of lung metastases—compact and loose—are formed following i.v. injection of tumor single cell suspensions. Since the compact tumors are almost always found surrounding tubular structures in the lungs (i.e. vessels and bronchies), we speculate that some tumor cells lodge in capillaries embedded in the rigid walls of these structures and that they grow there by expansion rather than infiltration, evident by the zone of compressed alveolar tissue often observed surrounding these tumors. Due to the paucity of vessels in these tumors, they may be nourished mainly by diffusion from the surrounding tissues. This is consistent with the fact that necrotic areas often develop in these

tumors when they reach a size of 200–300 microns. In contrast, the loose tumor nodules may develop from single tumor cells lodging into alveolar capillaries from where they initially may grow by expansion. However, due to the minimal amount of tissue in the alveolar walls, these tumors inevitably break through to the alveolar sacs, where they continue to grow, filling up sac after sac, apparently without much harm to the alveolar walls. This growth pattern explains why compression of the alveolar tissue is not seen around the loose tumors and why the density and, especially, the distribution of EMC and vascular components in the loose tumors is almost identical to that of normal lung alveolar tissue. This growth pattern of the loose tumors ensures them a rich blood supply—namely from the existing alveolar capillary network preserved in these tumors—and the loose tumors may continue to expand, in this manner, to a considerable size without the need of establishing their own blood-vascular support (necrotic areas are rarely found in even in very large tumors of loose morphology). In contrast, to be able to grow beyond a certain size, compact tumors must establish a vascular support (as a rule of thumb, tumors can only be nourished by diffusion alone until they grow to the size of approximately 200 microns from the nearest vessel [8, 9]). Preliminary data indicate that the compact tumors, over time, induce some neovascularization and develop into nodules of a mixed compact/loose phenotype. It is possible that the compact areas of these tumors can be nourished by pulmonary capillaries embedded in nearby parts of the tumor comprised of the loose type of tumor tissue. This raises the question to what extent anti-angiogenic treatment will be effective against lung malignancies containing tumor tissue of the loose phenotype, since the survival of the loose tumor tissue is not dependent on neovascularization. Indeed, while an anti-angiogenic factor of the VEGF family had significant anti tumor effect against subcutaneous B16-F10.P1 tumors (with rich neovascularization), the same treatment had no significant effect against neither loose, nor compact B16-F10.P1 lung tumors, indicating that neovascularization, at least initially, is not needed for the growth of these tumors (Lee and Basse, unpublished observations).

In conclusion, the ability of adoptively transferred A-NK cells to localize into lung metastases correlates with the morphology (compact or loose) of the metastases as well as their content of ECM and vasculature. While it is not fully understood how these factors interplay and what can be done to increase infiltration of the compact tumor tissue to improve cellular immunotherapy, we speculate that analysis of human tumor biopsies with respect to the density and distribution of these markers before treatment will indicate to what degree injected effector cells can be expected to localize to a patient's tumor(s) and may therefore help to select patients for cellular adoptive immunotherapeutic protocols.

**Acknowledgements** This study was supported by grants from the US-NIH (grants no. RO1CA87672 and R01CA104560) and the American Cancer Society (grant no. RPG-00-221-01-CDD) to



P.H.B and in part by the King Gustav V Jubilee Clinic Cancer Research Foundation to PA and UN. We thank Ms. Patricia Rice and Mrs. Lisa Bailey for excellent technical assistance.

## References

- Albertsson PA, Basse PH, Hokland M, Goldfarb RH, Nage-lkerke JF, Nannmark U, Kuppen PJ (2003) NK cells and the tumour microenvironment: implications for NK-cell function and anti-tumour activity. *Trends Immunol* 24:603–609
- Allavena P, Bianchi G, Paganin C, Giardina G, Mantovani A (1996) Regulation of adhesion and transendothelial migration of natural killer cells. *Nat Immun* 15:107–116
- Aonuma M, Saeki Y, Akimoto T, Nakayama Y, Hattori C, Yoshitake Y, Nishikawa K, Shibuya M, Tanaka NG (1999) Vascular endothelial growth factor overproduced by tumour cells acts predominantly as a potent angiogenic factor contributing to malignant progression. *Int J Exp Pathol* 80:271–281
- Basse P, Herberman RB, Nannmark U, Johansson BR, Hokland M, Wasserman K, Goldfarb RH (1991) Accumulation of adoptively transferred adherent, lymphokine-activated killer cells in murine metastases. *J Exp Med* 174:479–488
- Basse PH, Nannmark U, Johansson BR, Herberman RB, Goldfarb RH (1991) Establishment of cell-to-cell contact by adoptively transferred adherent lymphokine-activated killer cells with metastatic murine melanoma cells. *J Natl Cancer Inst* 83:944–950
- Burrows TD, King A, Loke YW (1995) The role of integrins in adhesion of decidual NK cells to extracellular matrix and decidual stromal cells. *Cell Immunol* 166:53–61
- Donskov F, Basse PH, Hokland M (1996) Expression and function of LFA-1 on A-NK and T-LAK cells: role in tumor target killing and migration into tumor tissue. *Nat Immun* 15:134–146
- Fidler IJ (2001) Regulation of neoplastic angiogenesis. *J Natl Cancer Inst Monogr* 28:10–14
- Gimbrone MA Jr, Cotran RS, Leapman SB, Folkman J (1974) Tumor growth and neovascularization: an experimental model using the rabbit cornea. *J Natl Cancer Inst* 52:413–427
- Gunji Y, Vujanovic NL, Hiserodt JC, Herberman RB, Gorelik E (1989) Generation and characterization of purified adherent lymphokine-activated killer cells in mice. *J Immunol* 142:1748–1754
- Guo P, Fang Q, Tao HQ, Schafer CA, Fenton BM, Ding I, Hu B, Cheng SY (2003) Overexpression of vascular endothelial growth factor by MCF-7 breast cancer cells promotes estrogen-independent tumor growth in vivo. *Cancer Res* 63:4684–4691
- Hokland M, Kjaergaard J, Kuppen PJ, Nannmark U, Agger R, Hokland P, Basse P (1999) Endogenous and adoptively transferred A-NK and T-LAK cells continuously accumulate within murine metastases up to 48 h after inoculation. *In Vivo* 13:199–204
- Kjaergaard J, Hokland M, Nannmark U, Hokland P, Basse P (1998) Infiltration patterns of short- and long-term cultured A-NK and T-LAK cells following adoptive immunotherapy. *Scand J Immunol* 47:532–540
- Kjaergaard J, Peng L, Cohen PA, Shu S (2003) Therapeutic efficacy of adoptive immunotherapy is predicated on in vivo antigen-specific proliferation of donor T cells. *Clin Immunol* 108:8–20
- Kjaergaard J, Shu S (1999) Tumor infiltration by adoptively transferred T cells is independent of immunologic specificity but requires down-regulation of L-selectin expression. *J Immunol* 163:751–759
- Kuppen PJ, Basse PH, Goldfarb RH, Van De Velde CJ, Fleuren GJ, Eggermont AM (1994) The infiltration of experimentally induced lung metastases of colon carcinoma CC531 by adoptively transferred interleukin-2-activated natural killer cells in Wag rats. *Int J Cancer* 56:574–579
- Macias C, Ballester JM, Hernandez P (2000) Expression and functional activity of the very late activation antigen-4 molecule on human natural killer cells in different states of activation. *Immunology* 100:77–83
- McLeskey SW, Tobias CA, Vezza PR, Filie AC, Kern FG, Hanfelt J (1998) Tumor growth of FGF or VEGF transfected MCF-7 breast carcinoma cells correlates with density of specific microvessels independent of the transfected angiogenic factor. *Am J Pathol* 153:1993–2006
- Melder RJ, Rosenfeld CS, Herberman RB, Whiteside TL (1989) Large-scale preparation of adherent lymphokine-activated killer (A-LAK) cells for adoptive immunotherapy in man. *Cancer Immunol Immunother* 29:67–73
- Nannmark U, Hokland ME, Agger R, Christiansen M, Kjaergaard J, Goldfarb RH, Bagge U, Unger M, Johansson BR, Albertsson PA, Basse PH (2000) Tumor blood supply and tumor localization by adoptively transferred IL-2 activated natural killer cells. *In Vivo* 14:651–658
- Nannmark U, Johansson BR, Bryant JL, Unger ML, Hokland ME, Goldfarb RH, Basse PH (1995) Microvessel origin and distribution in pulmonary metastases of B16 melanoma: implication for adoptive immunotherapy. *Cancer Res* 55:4627–4632
- Ribeiro U, Jr., Basse PH, Rosenstein M, Safatle-Ribeiro AV, Alhallak S, Goldfarb RH, Posner MC (1997) Retention of adoptively transferred interleukin-2-activated natural killer cells in tumor tissue. *Anticancer Res* 17:1115–1123
- Ribeiro U Jr, Whiteside TL, Basse PH, Safatle-Ribeiro AV, Huneke CE, Posner MC (1999) Activated natural killer cell tumor retention and cytokine production in colon tumor using a tissue-isolated model. *J Surg Res* 82:78–87
- Somersalo K (1996) Migratory functions of natural killer cells. *Nat Immun* 15:117–133
- van Deventer HW, Serody JS, McKinnon KP, Clements C, Brickey WJ, Ting JP (2002) Transfection of macrophage inflammatory protein 1 alpha into B16 F10 melanoma cells inhibits growth of pulmonary metastases but not subcutaneous tumors. *J Immunol* 169:1634–1639
- Vujanovic NL, Herberman RB, Maghazachi AA, Hiserodt JC (1988) Lymphokine-activated killer cells in rats. III. A simple method for the purification of large granular lymphocytes and their rapid expansion and conversion into lymphokine-activated killer cells. *J Exp Med* 167:15–29
- Yang Q, Hokland ME, Bryant JL, Zhang Y, Nannmark U, Watkins SC, Goldfarb RH, Herberman RB, Basse PH (2003) Tumor-localization by adoptively transferred, interleukin-2-activated NK cells leads to destruction of well-established lung metastases. *Int J Cancer* 105:512–519